The 12 May 2015 Kodari earthquake (M_w 7.3) in Central Nepal: delayed triggering by the 25 April 2015 Gorkha earthquake (M_w 7.8)

Rajeev Kumar Yadav[1], Bhaskar Kundu[2],*, Kalpna Gahalaut[1] and V. K. Gahalaut[3]

[1]CSIR-National Geophysical Research Institute, Hyderabad 500 007, India
[2]Department of Earth and Atmospheric Sciences, National Institute of Technology Rourkela, Rourkela 769 008, India
[3]National Centre for Seismology, Ministry of Earth Sciences, New Delhi 110 003, India

The 12 May 2015 earthquake of M_w 7.3 occurred in the Kodari region, Central Nepal, 17 days after the 25 April 2015 Gorkha earthquake (M_w 7.8) along the Himalayan plate boundary. Both the earthquakes were associated with predominantly thrust faulting on the Main Himalayan Thrust (MHT). This is the largest aftershock of the 2015 Gorkha earthquake which occurred approximately 150 km east of it. Our analysis suggests that the 2015 Gorkha earthquake significantly increased the Coulomb stress on the shallow unruptured and updip part of the MHT, further west of the 2015 rupture and also in the hypocentre region of 12 May 2015 M_w 7.3 aftershock. In the following 17 days period, Coulomb failure stress increased further by the relaxation of coseismic pore pressure on the eastern side of its coseismic rupture, where the 12 May 2015 aftershock had occurred.

Keywords: Coseismic rupture, delayed triggering, earthquakes, failure stress, thrust faulting.

AN earthquake has the potential to trigger another earthquake in the surrounding region in several ways, e.g. dynamic triggering during the passage of seismic waves through the fault zone, sudden change in static Coulomb failure stress (CFS); delayed triggering due to relaxation of coseismic stress either by poroelastic or viscoelastic relaxation effect, or through a combination of some or all of these factors. In case of delayed triggering, where the earthquake occurs a few days to a few weeks after the main shock, the poroelastic relaxation of coseismic stress is most prominent. In such cases redistribution of fluids, following the diffusion process, modifies the static stress on the critically stressed faults which results in the triggering of the earthquake with some time delay[1–4]. The occurrence of the 12 May 2015 Kodari earthquake (M_w 7.3), 17 days after the 25 April 2015 Gorkha earthquake, appears to be a perfect example of delayed triggering and we tested this hypothesis in this case (Figure 1).

A devastating earthquake with a moment magnitude of 7.8 struck Central Nepal on 25 April 2015, with its hypocentre located in the Gorkha district of Central Nepal[5]. The earthquake had initiated along the Main Himalayan Thrust (MHT), 80–100 km northwest of Kathmandu valley (Figure 1). It is the most destructive earthquake, since the 1934 Bihar–Nepal earthquake[6], causing extensive damage and high causalities (~8000)[7]; many historical structures collapsed in Kathmandu, including the great iconic Bhim Sen Tower. The earthquake focal mechanism and finite fault slip model from the United States Geological Survey (USGS) National Earthquake Information Centre (NEIC) indicate thrust motion on the subhorizontal fault plane with strike 295°, dip 10° and hypocentre depth of about 16.4 km which implies that it ruptured the MHT, without producing any primary surface rupture in the Himalayan region. However, palaeoseismological investigations suggest that several large Himalayan earthquakes ruptured the frontal part and their rupture reached the surface, e.g. the 1934, 1505 and 1255 earthquakes[8,9]. Thus unlike these historic events, this earthquake unzipped only the down-dip part of the locked portion of the MHT[7,10].

Globally recorded teleseismic P-waves study suggests that the rupture propagated southeastward from the hypocenter to about 160 km (ref. 11). Combined high-rate
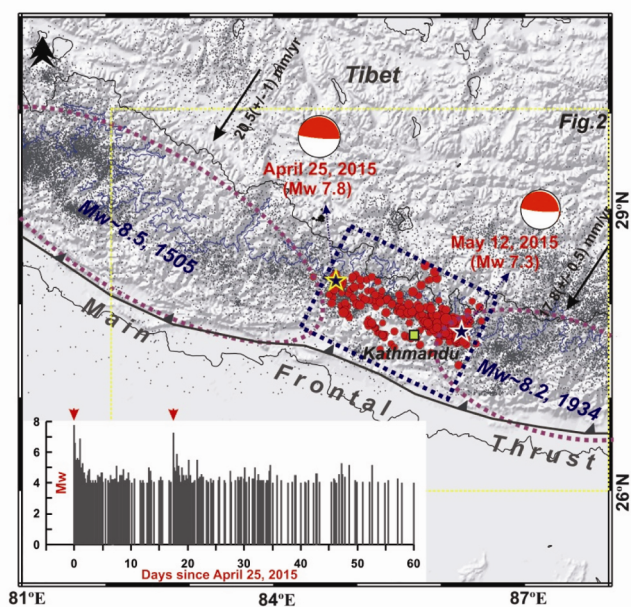

Figure 1. Seismotectonics of the region of the 25 April 2015 M_w 7.8 Gorkha earthquake. Epicentre of the 2015 Gorkha earthquake (yellow star) and its aftershocks (red circles) are from the National Seismic Centre (Nepal) and the epicentre of 12 May 2015 M_w = 7.3 earthquake (white star). Convergence rate (black arrows) across the Himalaya are from Ader *et al.*[27]. Grey dots show mid-crustal seismicity between 1995 and 2008 from the National Seismic Centre (DMG, Nepal). Blue contour represents 3500 m elevation that approximately marks the downdip edge of locked zone in the Himalayan detachment. Approximate rupture locations of the historic events in Nepal since 1505 are shown by ellipses. Yellow rectangle marks the region considered in Figure 2.

*For correspondence. (e-mail: rilbhaskar@gmail.com)

GPS and InSAR data suggest that the earthquake ruptured as a slip pulse of ~20 km width, ~6 sec duration, and with peak sliding velocity of 1.1 m/s that propagated towards Kathmandu basin at ~3.3 km/s over ~140 km (ref. 7). Several GPS sites in Nepal and southern China showed coseismic offset caused by the earthquake[12]. Four GPS sites in the Indian region, immediately to the south of the rupture, showed significant coseismic horizontal offsets ranging between 3 and 7 mm towards north[12]. The aftershock distribution, including several seismic events of $>M_w$ 5.5, extended east of the hypocentre of the mainshock, and a M_w 7.3 aftershock occurred in Kodari region, Central Nepal, approximately 150 km east of the hypocentre of the main shock (Figure 1). So far this is the largest aftershock of the earthquake which occurred 17 days after the main shock and with predominant thrust fault and focal depth of 19.5 km (refs 13, 14).

Occurrences of the 2015 Gorkha and Kodari earthquakes have raised a few crucial points: (1) A question of immediate concern is whether and how the Gorkha earthquake would influence the regional seismicity. A more specific question is whether the 12 May 2015 Kodari earthquake (M_w 7.3), which is located about 150 km southeast from the main shock and which occurred 17 days after the Gorkha earthquake (Figure 1), was a delayed triggered event. (2) Probability of occurrence of high-magnitude earthquakes on the locked patches of the MHT, up-dip and further west of the 2015 rupture might have increased due to increase in static stress caused by the 2015 Gorkha earthquake. (3) The rupture did not propagate towards west, possibly indicating the presence of an aseismic or structural barrier[10,15]. (4) Rupture of this earthquake partly overlapped the down-dip portion of the 1934 Bihar–Nepal earthquake rupture, possibly implying that the down-dip segment of the MHT did not rupture or did not release strain fully, during the 1934 earthquake. Some of these issues may be solved through modelling and their validity would be tested with time in case of occurrence of a future earthquake in the neighbourhood of the 2015 Gorkha earthquake. However, the issue of the 12 May 2015 Kodari earthquake being a delayed triggered event can be tested easily. In this communication, we resolve this by computing Coulomb stress and its poroelastic relaxation considering various available rupture models of the mainshock.

Occurrence of a triggered event largely depends on nature of coseismic stresses. Various models of coseismic slip during an earthquake would produce different effects. Hence it is important to consider all possible models of rupture. In case of the 2015 Gorkha earthquake, we considered six available rupture models (referred as M(A) for Avouac *et al.*[10], M(G) for Galetzka *et al.*[7], M(Y1) for Yadav *et al.*[12], M(U) for USGS[5], M(W) for Wang and Fialko[16] and M(Y2) for Yagi and Okuwaki[17]). Almost all rupture models have been derived using seismic waveforms recorded at teleseismic stations, seismic back-

projection approach, InSAR and image correlation techniques and GPS data (both high rate and 30 s). Although these models are similar in a broad sense, they differ in terms of details of slip distribution.

Yadav *et al.*[12] considered all these coseismic rupture models and compared the average misfit in each case for both near and far-field GPS sites. Their model provided the least misfit between the coseismic offsets derived from GPS measurements (30 s) and the simulated coseismic displacement at near-field and far-field sites (i.e. including few GPS sites from the Indo-Gangetic Plains). Models which include InSAR data, seismic back-projection and high rate GPS data can provide more constraints on the spatial complexity of the rupture propagation process. However, models based on InSAR technique may also contain some effect of post-seismic deformation that is difficult to remove. Moreover, each methods/technique has its inherent limitations. Therefore, it is difficult to claim which is the best coseismic rupture model amongst the six available for the main shock. However, it may be noted that all rupture models appear similar and constrain large slip (about 6 m) between the epicentres of the mainshock and its largest aftershock of 12 May 2015, slightly north of Kathmandu valley.

The static CFS caused by slip dislocation patches in homogeneous elastic half-space considering the above coseismic rupture models was computed using the Coulomb 3.3 code[18]. Interestingly, in all cases the occurrence of this earthquake significantly increased the Coulomb stress on the adjoining locked portions of the MHT in the updip (i.e. frontal arc region) and farther west of the coseismic rupture (Figure 2). This aspect has been pointed out by the earlier workers as well[10,13,19]. However, even after more than a year, no significant earthquake has occurred in this region. It could be that the stress in the region has not reached to a critical level, either due possibly to weak rheology, low stress conditions or structural controls[10,13]. Patterns of CFS changes farther east of the coseismic rupture and on the hypocentre region of the 12 May 2015 earthquake are complicated. We observed positive CFS change corresponding to almost all coseismic rupture models, namely M(G), M(Y1), M(W), M(U) and M(Y2), however, rupture model M(A), imparted negative CFS change in the region at a depth of 15 km (Figure 2). If we consider the earth to be perfectly elastic with no diffusion and no significant increase in the interseismic strain accumulation, then all aftershocks, including the 12 May 2015 event in the Kodari region, should have occurred immediately after the main shock. It may be noted that with the present rate of slip deficit of ~2 cm/yr in Nepal Himalaya, stress increase due to interseismic strain accumulation would be only ~0.002 bar in the 17 days period, which is insignificant[20]. A delayed occurrence of the aftershocks with decreasing frequency hints at the relaxation of stress, which modified the stress in the region. At such a short time interval, poroelastic
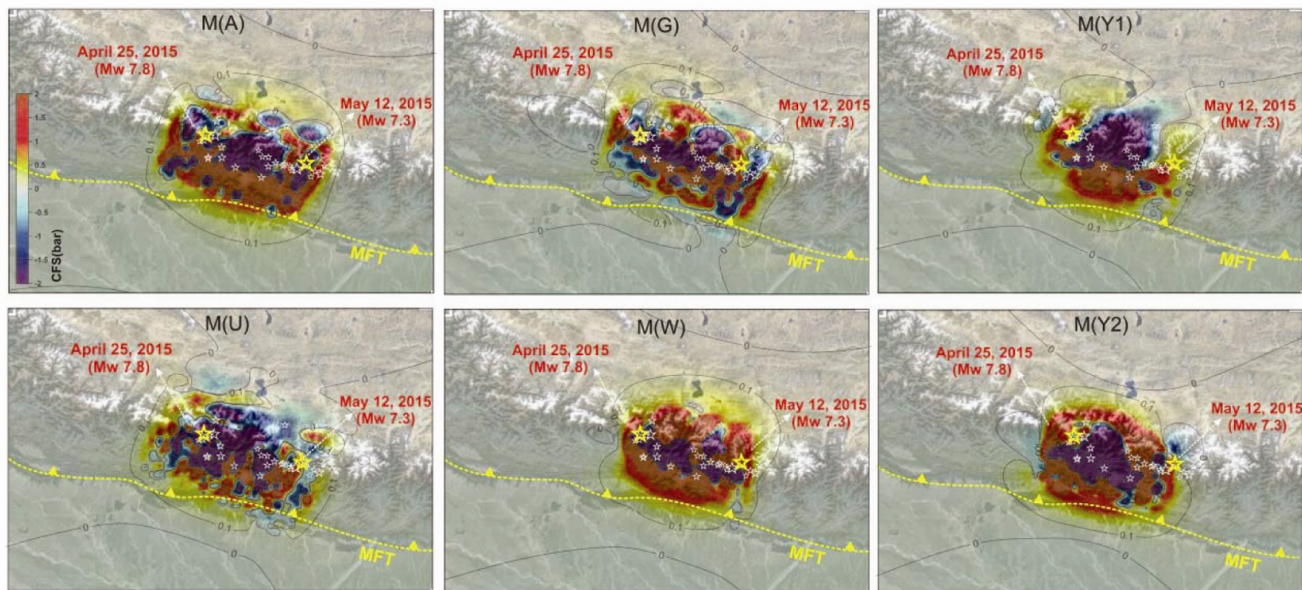
Figure 2. Coulomb failure stress change (bars) on the Himalayan detachment (15 km depth) caused by the 25 April 2015 Gorkha earthquake, using different rupture models namely M(A), M(G), M(Y1), M(U), M(W) and M(Y2) (see text for discussion). Stars represent epicentre locations of the 25 April 2015 and 12 May 2015 earthquakes. MFT, Main Frontal Thrust.

relaxation, due to redistribution of fluids may be considered as the possible mechanism[2–4]. Viscoelastic relaxation occurs over a longer period and may not be applicable here.

To understand the mechanical relationship between these two earthquakes (25 April 2015 Gorkha earthquake and 12 May 2015, M_w 7.3 aftershock), we followed that analytical approach of Gahalaut *et al.*[2] and computed the poroelastic relaxation of coseismic pore pressure and modified postseismic Coulomb stress in the surrounding volume containing the MHT. The ultimate assumption of this modelling is that the stress–strain relationship is governed by linear, undrained poroelasticity and the flow of fluids in the porous crust follows the mass diffusion law described by Darcy's law[21]. To compute the spatio-temporal variation of pore pressure [$p(x, y, z)$] at a point (x, y, z) at time (t) due to poroelastic relaxation of coseismic pore pressure (p_c), we used the Green's function solution of inhomogeneous diffusion equation proposed by Kalpna and Chander[22] which is represented as follows

$$p(x,y,z,t) = \int_0^\infty \int_{-\infty}^{\infty} \int_{\infty}^{-\infty} p_c(x',y',z') G \, \mathrm{d}z' \, \mathrm{d}y' \, \mathrm{d}x',$$

where G, the Green's function and p_c are expressed as

$$G(x,y,z,x',y',z',t)$$

$$= \frac{1}{8[\pi ct]^{3/2}} \left[\mathrm{e}^{-\frac{(z-z')^2}{4ct}} - \mathrm{e}^{-\frac{(z+z')^2}{4ct}} \right] \times \mathrm{e}^{-\left[\frac{(y-y')^2+(x-x')^2}{4ct} \right]}$$

$$p_c = B \frac{\theta}{3},$$

where c is the hydraulic diffusivity, B the Skempton's coefficient, and $\theta/3$ is the mean normal stress. Our specific interest is to quantify the change in CFS [$\Delta\mathrm{CFS} = \Delta\tau - \mu(\Delta\sigma - \Delta p)$] due to the relaxation of coseismic pore pressure of the 25 April 2015 Gorkha earthquake to the east of its coseismic rupture, where the 12 May 2015 Kodari aftershock occurred. In this expression, μ is the frictional coefficient and Δ represents change in normal stress (σ), shear stress (τ) and pore pressure (p). Positive $\Delta\mathrm{CFS}$ change encourages failure on the critically stressed fault system and vice versa. We considered all available coseismic rupture models of the 2015 Gorkha earthquake. We used undrained Poisson's ratio as 0.25, c in the range 3–10 m²/s, B as 1, and μ in the range 0.20–0.65 that allowed a satisfactory fit to the data in case of triggered seismicity[2,3,23–26].

As mentioned earlier, there is a significant difference in static $\Delta\mathrm{CFS}$ in the hypocentre region of the 12 May 2015 earthquake derived from various rupture models. Thus accordingly coseismic pore pressure-induced stress relaxation and its temporal evolution are also different with respect to spatio-temporal evolution of pore pressure change at the hypocentre of the 12 May 2015 earthquake (Figure 4). For poroelastic stress relaxation and delayed triggering process, one condition is crucial – the triggering region must be in the coseismic dilatation zone, where pore pressure must increase significantly after the occurrence of the main earthquake. It has been noticed
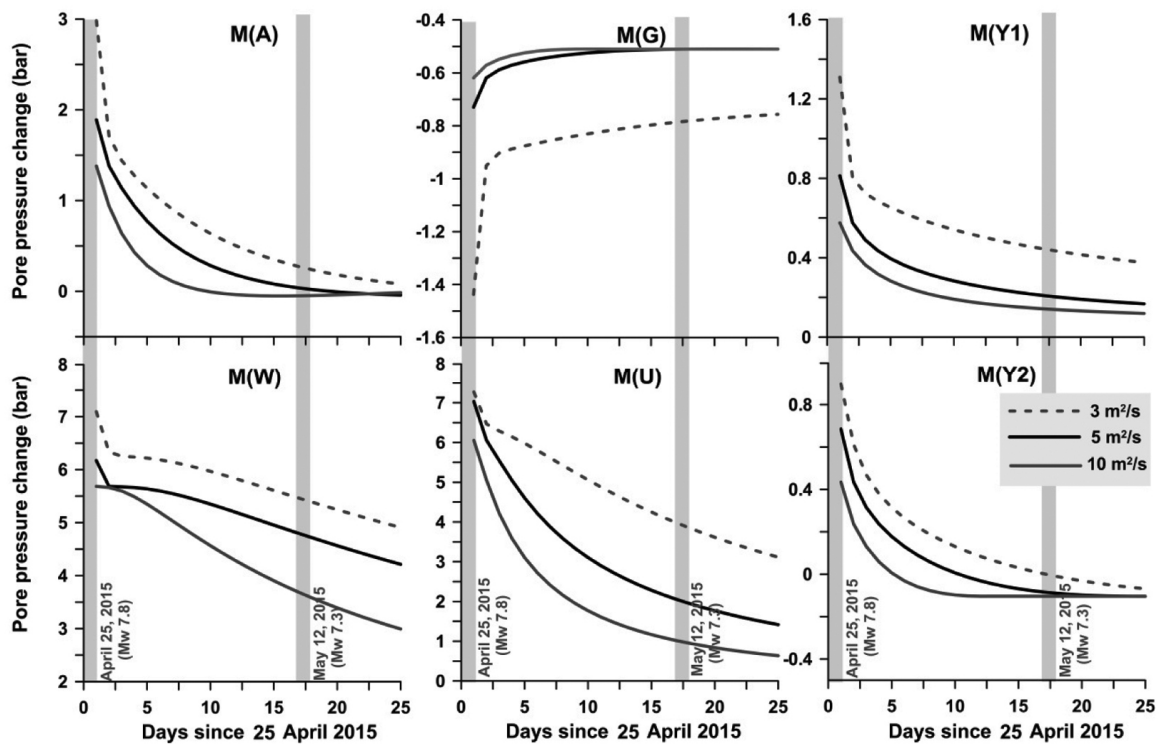
Figure 3. Temporal evolution of pore pressure change at the hypocentre of the 12 May 2015 earthquake (M_w 7.3) in Central Nepal region at 15 km depth, using different rupture models (M(A) to M(Y2)), and different hydraulic diffusivity values (3, 5 and 10 m^2/s). Note rupture model M(G) shows significant increase in pore pressure after the 2015 Gorkha earthquake.

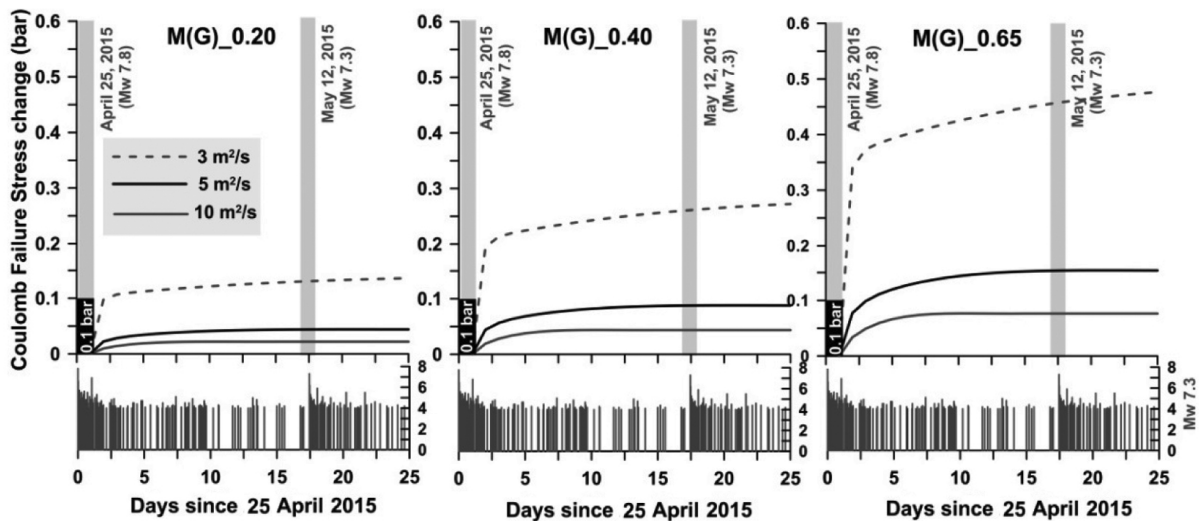**Figure 4.** Temporal evolution of Coulomb failure stress change (bar) at the hypocentre of the 12 May 2015 earthquake (M_w 7.3) in Central Nepal region at 15 km depth using rupture model M(G), for different hydraulic diffusivity values (3, 5 and 10 m^2/s) and different coefficients of friction (0.2, first panel; 0.4, second panel and 0.65, third panel).

that only the coseismic rupture model M(G) qualifies this critical criterion. All the remaining models show decrease in pore pressure after the occurrence of the main shock (Figure 5). Therefore, in the subsequent period of 17 days after the 2015 Gorkha earthquake, pore pressure in-creased in the hypocentre region of the 12 May 2015 M_w 7.3 aftershock, which further decreased the effective normal stress and increased CFS (Figure 5). Thus it appears that the 12 May 2015 Kodari event was possibly a delayed triggered aftershock of the 25 April 2015 Gorkha
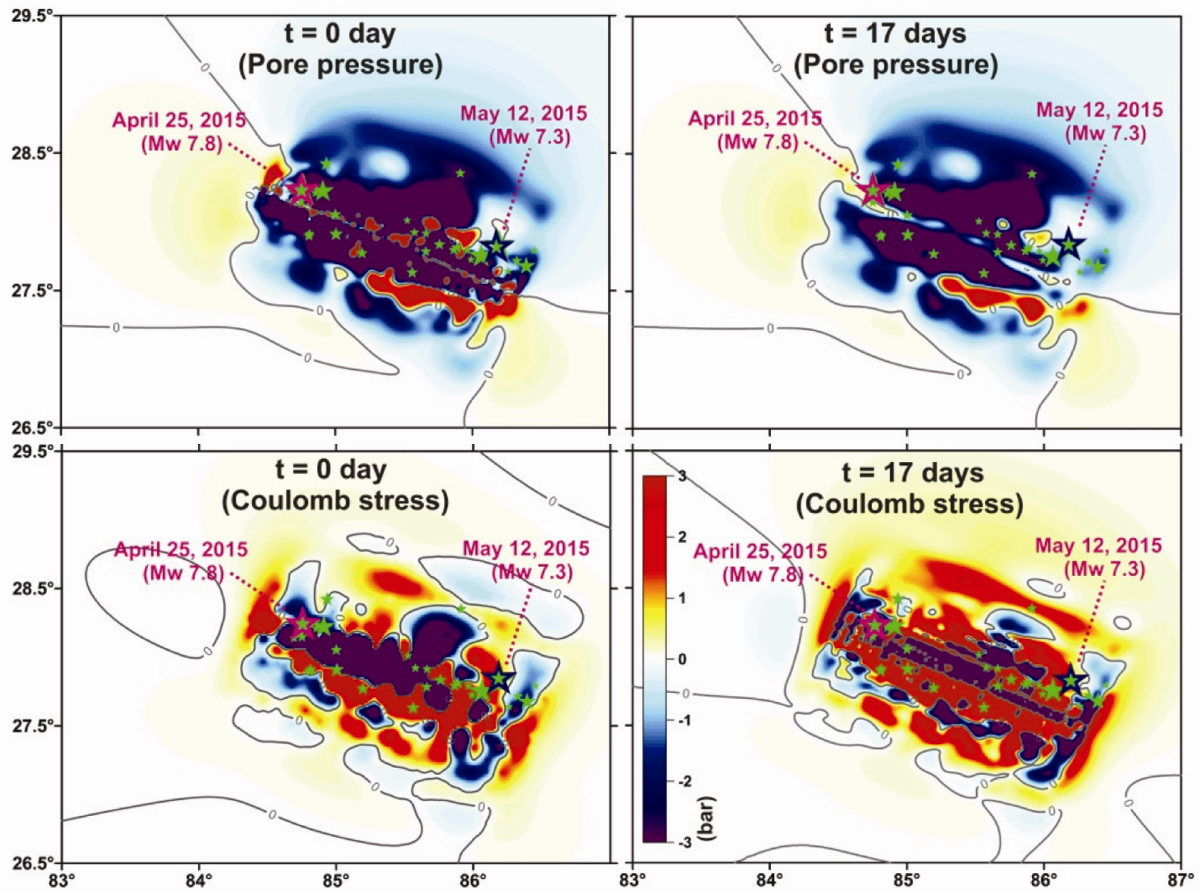
Figure 5. Correlation between 2015 Gorkha aftershocks ($M_w > 5.5$, epicentre locations are from Adhikari *et al.*[28]) and spatio-temporal variation of pore pressure due to poroelastic relaxation (shown in the upper two panels), and postseismic Coulomb stresses (shown in the lower two panels) at 15 km depth. Note the increase in Coulomb stress in the lower right panel.
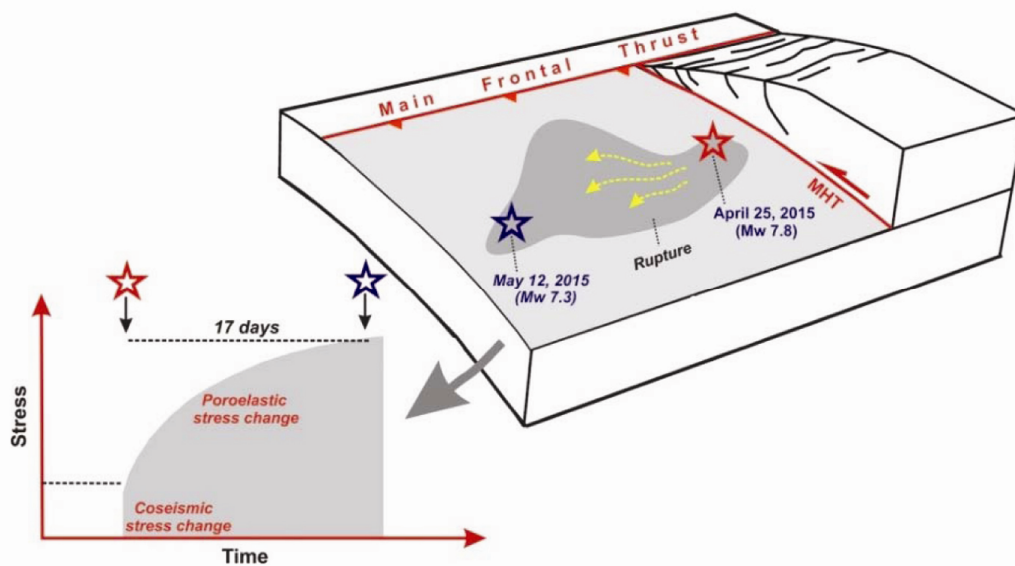

Figure 6. Conceptual model for the mechanism of the 12 May 2015 earthquake in Central Nepal triggered by the pore pressure relaxation of the coseismic stress due to the 25 April 2015 Gorkha earthquake. MHT, Main Himalayan Thrust.

earthquake. The coseismic stress change caused by the main shock significantly increased due to poroelastic relaxation and reached a critical level, which triggered the Kodari event (Figure 6).

Another conclusion which can be drawn here is that all the models suggest that the occurrence of these earthquakes certainly increased stress on the up-dip part of the MHT, i.e. south of the rupture and on the western part of the MHT. This must have increased the probability of earthquake occurrence in these two regions.

From the above analysis we summarize the following points (Figure 6): (1) The 12 May 2015 earthquake of M_w 7.3 in the Kodari region, Central Nepal can be considered as delayed triggered aftershock of the 2015 Gorkha earthquake of M_w 7.8. The coseismic stresses increased due to pore pressure redistribution, highlighting the poroelastic relaxation of coseismic stress. (2) Probability of occurrence of large earthquakes on the locked patches of the MHT updip and farther west of the 2015 rupture has increased significantly as stress regime has been raised well above the triggering thresholds due to the 2015 Gorkha earthquake. This result is consistent for all slip models.

1. Freed, A. and Lin, J., Accelerated stress buildup on the southern San Andreas fault and surrounding regions caused by Mojave Desert earthquakes. *Geology*, 2002, **30**, 571–574.

2. Gahalaut, K., Gahalaut, V. K. and Kayal, J. R., Poroelastic relaxation and aftershocks of the 2001 Bhuj earthquake, India. *Tectonophysics*, 2008, **460**, 76–82; doi:10.1016/j.tecto.2008.07.004.

3. He, J. and Peltzer, G., Poroelastic triggering in the 9–22 January 2008 Nima Gaize (Tibet) earthquake sequence. *Geology*, 2010, **10**, 907–910; doi:10.1130/G31104.1.

4. Kundu, B. *et al.*, The 2005 volcano-tectonic earthquake swarm in the Andaman Sea: triggered by the 2004 great Sumatra–Andaman earthquake. *Tectonics*, 2012, **31**, TC5009; doi:10.1029/2012-TC003138.

5. US Geological Survey, 2015; http://earthquake.usgs.gov/earthquakes/eventpage/us20002926#scientific_finitefault

6. Bilham, R., Earthquakes in India and the Himalaya: tectonics, geodesy and history. *Ann. Geophys.*, 2004, **47**(2–3), 839–858.

7. Galetzka, J. *et al.*, Slip pulse and resonance of Kathmandu basin during the 2015 M_w 7.8 Gorkha earthquake, Nepal imaged with geodesy. *Science*, 2015, **349**, 1091–1095.

8. Lavé, J., Yule, D., Sapkota, S., Basant, K., Madden, C., Attal, M. and Pandey, R., Evidence for a great medieval earthquake (approximate to 1100 AD) in the central Himalayas, Nepal. *Science*, 2005, **307**, 1302–1305.

9. Kumar, S., Wesnousky, S. G., Rockwell, T. K., Briggs, R. W., Thakur, V. C. and Jayangondaperumal, R., Paleoseismic evidence of great surface rupture earthquakes along the Indian Himalaya. *J. Geophys. Res.*, 2006, **111**, B03304; doi:10.1029/2004JB003309.

10. Avouac, J.-P., Meng, L., Wei, S., Wang, T. and Ampuero, J.-P., Lower edge of locked Main Himalayan Thrust unzipped by the 2015 Gorkha earthquake. *Nature Geosci.*, 2015, **8**, 708–711; doi:10.1038/NGEO2518.

11. Fan, W. and Shearer, P. M., Detailed rupture imaging of the 25 April 2015 Nepal earthquake using teleseismic *P* waves. *Geophys. Res. Lett.*, 2015; doi:10.1002/2015GL064587.

12. Yadav, R. K. *et al.*, Rupture model of M_w 7.8 2015 Gorkha, Nepal earthquake: constraints from GPS measurements of coseismic offsets. *J. Asian Earth Sci.*, 2017, **133**, 56–61.

13. Bai, L., Liu, H., Ritsema, J., Mori, J., Zhang, T., Ishikawa, Y. and Li, G., Faulting structure above the Main Himalayan Thrust as shown by relocated aftershocks of the 2015 M_w 7.8 Gorkha, Nepal earthquake. *Geophys. Res. Lett.*, 2016, **43**, 637–642; doi:10.1002/2015GL066473.

14. Duputel, Z., Vergne, J., Rivera, L., Wittlinger, G., Farra, V. and Hetényi, G., The 2015 Gorkha earthquake: a large event illuminating the Main Himalayan Thrust fault. *Geophys. Res. Lett.*, 2016, **43**, 2517–2525; doi:10.1002/2016GL068083.

15. Hubbard, J. *et al.*, Structural segmentation controlled the 2015 M_w 7.8 Gorkha earthquake rupture in Nepal. *Geology*, 2016, **44**(8), 639–642.

16. Wang, K. and Fialko, Y., Slip model of the 2015 M_w 7.8 Gorkha (Nepal) earthquake from inversion of ALOS-2 and GPS data. *Geophys. Res. Lett.*, 2015; doi:10.1002/2015GL065201.

17. Yagi, Y. and Okuwaki, R., Integrated seismic source model of the 2015 Gorkha, Nepal, earthquake. *Geophys. Res. Lett.*, 2015, **42**, 6229–6235; doi:10.1002/2015GL064995.

18. Toda, S., Stein, R. S., Sevilgen, V. and Lin, J., Coulomb version 3.3 Graphic-rich deformation and stress-change software for earthquake, tectonic, and volcano research and teaching – user guide. US Geological Survey Open-File Report, Earthquake Science Center, Menlo Park Science Center, Menlo Park, California, USA, 2011, p. 63.

19. Lui, C. *et al.*, Rupture processes of the 2015 M_w 7.9 Gorkha earthquake and its M_w 7.3 aftershock and their implications on the seismic risk. *Tectonophysics*, 2016, **682**, 264–277.

20. Cattin, R. and Avouac, J.-P., Modeling of mountain building and the seismic cycle in the Himalaya of Nepal. *J. Geophys. Res.*, 2000, **105**, 13,389–13,407.

21. Wang, H. F., *Theory of Linear Poroelasticity*, Princeton University Press, Princeton, NJ, USA, 2000, p. 287.

22. Kalpna and Chander, R., Green's function based stress diffusion solutions in the porous elastic half space for the time varying finite reservoir loads. *Phys. Earth Planet. Int.*, 2000, **120**, 93–101.

23. Talwani, P., Chen, L. and Gahalaut, K., Seismogenic permeability. *J. Geophys. Res.*, 2007, **112**, B07309; doi:10.1029/2006JB004665.

24. Peltzer, G., Rosen, P., Rogez, F. and Hudnut, K., Poroelastic rebound along the Landers 1992 earthquake surface rupture. *J. Geophys. Res.*, 1998, **103**, 30,131–30,145; doi:10.1029/98JB02302.

25. Cocco, M. and Rice, J., Pore pressure and poroelasticity effects in Coulomb stress analysis of earthquake interactions. *J. Geophys. Res.*, 2002, **107**(B2); doi:10.1029/2000JB000138.

26. Talwani, P. and Acree, S., Pore pressure diffusion and the mechanism of reservoir induced seismicity. *Pure Appl. Geophys.*, 1984, **122**, 947–965; doi:10.1007/BF00876395.

27. Ader, T. *et al.*, Convergence rate across the Nepal Himalaya and interseismic coupling on the Main Himalayan Thrust: Implications for seismic hazard. *J. Geophys. Res.*, 2012, **117**(B4), b04403; doi:10.1029/2011JB009071.

28. Adhikari, L. B. *et al.*, The aftershock sequence of the 2015 April 25 Gorkha–Nepal earthquake. *Geophys. J. Int.*, 2015, **203**(3), 2119–2124.